Conformational Switching of a Foldamer in a Multicomponent System by pH-Filtered Selection between Competing Noncovalent Interactions

Julien Brioche,[†] Sarah J. Pike,[†] Sofja Tshepelevitsh,[‡] Ivo Leito,[‡] Gareth A. Morris,[†] Simon J. Webb,[†,§] and Jonathan Clayden*[,†]

[†]School of Chemistry, University of Manchester, Oxford Road, Manchester M13 9PL, United Kingdom
[‡]Institute of Chemistry, University of Tartu, Ravila 14a, Tartu 50411, Estonia
[§]Manchester Institute of Biotechnology, University of Manchester, 131 Princess Street, Manchester M1 7DN, United Kingdom

Ⓢ *Supporting Information*

ABSTRACT: Biomolecular systems are able to respond to their chemical environment through reversible, selective, noncovalent intermolecular interactions. Typically, these interactions induce conformational changes that initiate a signaling cascade, allowing the regulation of biochemical pathways. In this work, we describe an artificial molecular system that mimics this ability to translate selective noncovalent interactions into reversible conformational changes. An achiral but helical foldamer carrying a basic binding site interacts selectively with the most acidic member of a suite of chiral ligands. As a consequence of this noncovalent interaction, a global absolute screw sense preference, detectable by ^{13}C NMR, is induced in the foldamer. Addition of base, or acid, to the mixture of ligands competitively modulates their interaction with the binding site, and reversibly switches the foldamer chain between its left and right-handed conformations. As a result, the foldamer–ligand mixture behaves as a biomimetic chemical system with emergent properties, functioning as a "proton-counting" molecular device capable of providing a tunable, pH-dependent conformational response to its environment.
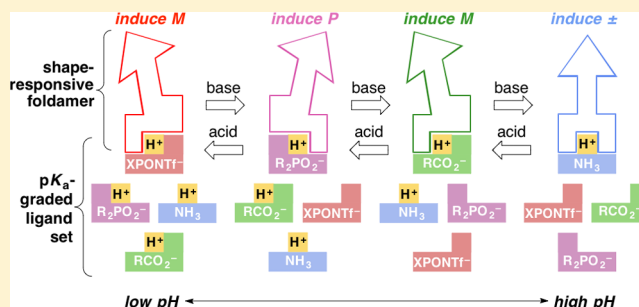
■ INTRODUCTION

A defining difference between biological and chemical systems lies in biology's ability to store, process, and amplify information in the midst of immense chemical complexity.[1−4] The remarkable selectivity displayed by biomolecules in their binding of other biomolecules, ligands, or metabolites allows the simultaneous independent but interactive control of numerous chemical signaling pathways. As a result, multiple biochemical processes may be controlled, all taking place within the same physical phase.[5] Communication events in biological systems typically couple selective molecular recognition to some form of conformational response,[6−9] allowing modulation of function in a peptide, protein, or nucleic acid. Classic examples[10] include G-protein coupled receptors, which modify their conformation in response to the binding of an extracellular ligand, and the allosteric protein hemoglobin,[11,12] which adjusts its conformation on binding of oxygen, and phosphorylases.[13] Other proteins exhibit pH-dependent conformational switching.[14,15] Signaling pathways result when further biochemical events are initiated as a consequence of these conformational changes—the release of GDP into a cell, further cooperative binding of oxygen, or phosphorylation of active hydroxyl groups.

This relay of information through reversible conformational changes may be mimicked[16−20] by artificial, conformationally defined extended molecular structures (foldamers[21−23]) that adjust their global conformational preference as a result of the reversible covalent binding of a ligand. Three-dimensional structural information about the ligand is thus transmitted from a binding site in the artificial receptor to a remote reporter group.[24] However, in a real biological system, every binding site is continually buffeted by a menagerie of potential ligands, among which it must recognize and bind a suitable partner, leading to a corresponding selective conformational response.

We now report a receptor mimic that incorporates a basic binding site, whose conformational preference is reversibly modulated by selective noncovalent interactions. When several alternative acidic ligands are presented simultaneously to the receptor, its response is dictated by the ligands' pK_a- and pH-dependent binding ability. The receptor's tunably selective response to the ligand is communicated conformationally to a remote site in the molecule, where the resulting global conformational preference is revealed by NMR. Through a characteristic combination of noncovalent ion-pairing and

hydrogen-bonding interactions, each potential ligand induces a quantitatively different, spectroscopically quantifiable, conformational preference in the receptor mimic. Cycling between conformational outputs is made possible by the selective activation or silencing of ligands by varying the pH (and hence protonation state) of the system. The multicomponent mixture of ligands plus the receptor thus constitutes a chemical system with emergent properties, functioning as a device capable of counting[25,26] protons and providing a tunable, conformationally encoded output.

RESULTS AND DISCUSSION

Identifying a Versatile Binding Site. Conformational change induced by noncovalent binding of a ligand is a well established feature of supramolecular systems.[27−36] In the context of extended dynamically switchable helical foldamer structures,[37−41] Inai and co-workers showed[42−45] that a noncovalent interaction between an enantiopure N-protected α-amino acid and the free amino terminus of an achiral but helical polyamide is capable of eliciting a circular dichroism (CD) response from the foldamer, indicating the induction of some degree of screw-sense preference in the helical structure.[39,46] The perturbation of the equilibrium between the left- and right-handed conformers arises from a combination of localized ion pairing and hydrogen bonding interactions in a 1:1 complex between the carboxylic acid and the foldamer.[47] Nonetheless, excess ligand produced complexes with higher stoichiometry that interfered with the conformational responses.[47] Building on Inai's work, we aimed first to quantify the screw-sense preference induced in a conformationally labile foldamer as a result of noncovalent hydrogen bonding/ion pairing interactions, and second to identify a more versatile basic binding site that would be able to maintain selective and strong 1:1 binding interactions even in the presence of a mixture of different competing ligands.

Because of their well established ability to form conformationally uniform,[48] hydrogen-bonded 3_{10}-helical structures[49−54] in a range of solvents, we used foldamers consisting of oligomers of 2-aminoisobutyric acid (Aib) residues. Helical Aib oligomers are achiral, and therefore necessarily conformationally racemic, but may be induced to adopt a globally preferred screw sense (left-handed M or right-handed P) by a covalently attached terminal chiral residue.[55−61]

A small library of potential binding sites **B0−7** were ligated to the N-terminus of 4−9 Aib residue oligomers to form achiral helical foldamers (**F0−7**) (for synthetic details, see the Supporting Information, SI). Several chiral acids (**HA1−6**)[62] or anions (**A7⁻**, **A8⁻**)[63,64] with a range of gross structural features and pK_a values were chosen as potential chiral ligands (Figure 1).[65,66] To allow us to quantify the global conformational change in any of **F0−F7** induced by interaction with any of **HA1−6**, a ^{13}C NMR reporter of helical screw-sense preference was incorporated into the foldamers **F0−7** at a position remote from the binding site. The C-terminal Aib residue was labeled with ^{13}C at both enantiotopic methyl groups.[67] At ambient temperature under normal conditions of rapid screw sense inversion, the anisochronicity ($\Delta\delta$) of the two diastereotopic ^{13}CH$_3$ signals of the NMR probe is proportional to the imbalance between the population of M and P conformers of the foldamer **F** (the helical excess, h.e.).[58] The anisochronicity $\Delta\delta$ was typically measured by recording ^{13}C NMR spectra at 296 K in CDCl$_3$ of mixtures of **HA** and **F** at concentration of [**F**] = 10 mM (sufficiently low to avoid
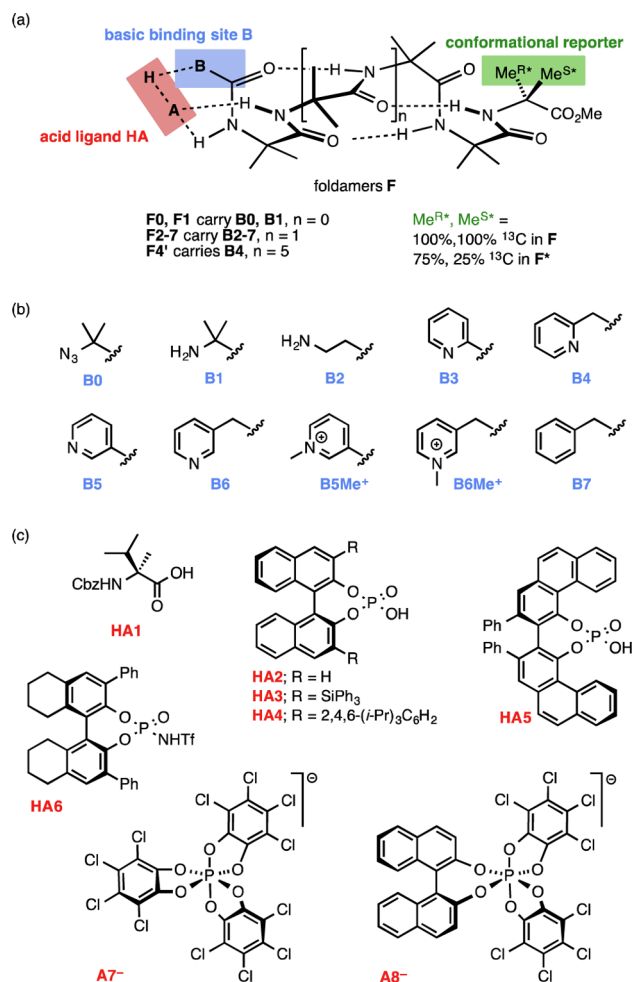

Figure 1. (a) Achiral foldamers; (b) binding sites; and (c) chiral acids and anions.

foldamer aggregation[68]) and in a ratio **HA:F** = 1.2:1. The values of $\Delta\delta$ are reported in Table 1 as anisochronicity (in ppb) and as a screw-sense preference (helical excess, h.e.) calculated from $\Delta\delta$ as described in the SI.[59]

Quantifying the Effect of Ligands. Initial experiments employed primary amine binding sites **B1** and **B2**[47] (Table 1, entries 1, 2). In the case of free Aib-terminated **F1**, carboxylic acid **HA1** and N-triflyl phosphoramide **HA6** failed to induce a screw-sense preference in the achiral foldamer ($\Delta\delta$ = 0). However, phosphoric acids **HA2−HA5** induced a conformational preference in **F1** having a maximum value of 70% h.e. for **HA5** (entry 1). With **F2**, which contains a β-alanine binding site, all of **HA1−HA6** induced at least some conformational preference in **F2** (entry 2), with a maximum value of 63% h.e. for **HA4**. The parent, nonbasic azido-substituted foldamer (entry 0) displayed almost no conformational induction with **HA1**, **HA4**, or **HA6**, showing that nonspecific interactions of **HA** with the Aib oligomer were insignificant.

Inai had shown that N-terminal β-alanine-bearing foldamers participate with N-Boc protected amino acids in stable 1:1 interactions which retain their conformational preference in the presence of moderate excesses of the amino acid.[47] However, we found that this was not the case for the β-alanine-capped foldamer−phosphoric acid pair **HA4↔F2**: in this case, both the ratio **HA4:F2** and the concentration [**F2**] had a significant effect on the conformational preference of the helical foldamer.

Table 1. Measured Anisochronicity (^{13}C NMR in CDCl$_3$, 296 K) and Calculated Helical Excess Induced at the Remote Terminus of Foldamers F by Interaction with HA ([F] = 10 mM; [HA] = 12 mM (1.2 Equiv) unless Indicated Otherwise)

entry	foldamer F	$n =$	binding site B	anisochronicity ($\Delta\delta$, ppb) and helical excess (%, in brackets) induced in F by HA (1.2 equiv.)							
				HA1[a]	HA2	HA3	HA4	HA5	HA6	A7[-f]	A8[-f]
0	**F0**	0	**B0**	0	–	–	58 (3)	–	40 (2)	–	–
1	**F1**	0	**B1**	0	525 (30)	88 (5)	500 (28)	1236 (70)	0	–	–
2	**F2**	1	**B2**	124 (7)	105 (6)	131 (7)	1127 (63)	171 (10)	55 (3)	–	–
3	**F3**	1	**B3**	0	99 (5)	0	116 (6)	102 (6)	37 (2)	–	–
4	**F4**	1	**B4**	838 (47)	88 (5)	306 (17)	1035 (58)	234 (13)	102 (6)	–	–
5	**F4'**	5	**B4**	783 (44)	–	–	1068 (60)	–	73 (4)	–	–
6	**F6**	1	**B6**	33 (2)	22 (1)	127 (7)	492 (27)	237 (13)	169 (10)	–	–
7	**F5Me$^+$**	1	**B5Me$^+$**	–	–	–	–	–	–	(20)[b,c]	(28)[b,c]
8	**F6Me$^+$**	1	**B6Me$^+$**	–	–	–	–	–	–	0[b,d]	(12)[b,e]
9	**F7**	1	**B7**	0	–	–	26 (1)	–	0	–	–

Entries shaded in grey indicate the greatest levels of non-covalent conformational induction, and these combinations were used further in later experiments. [a]Measured using 1.5 equiv HA. [b]Using a ^{19}F NMR-based probe. [c]8 equiv. A$^-$. [d]10 equiv. A$^-$. [e]4 equiv. A$^-$. [f]In the presence of 28 vol % methanol; empty table cell, value not measured.

Anisochronicity ($\Delta\delta$) measured in **F2** increased with the amount of **HA4** up to a maximum value corresponding to ca. 70% h.e. at 1:1 **HA4:F2** but then decreased in the presence of excess **HA4** dropping to 56% h.e. with 2.5 equiv. **HA4** (SI Figure S34). Conformational control in the **HA4↔F2** mixture was also concentration-dependent, increasing in a linear manner up to a concentration [**F2**] = 2.5 mM and then dropping (SI Figure S48).

Phosphoric acids **HA2−5** and *N*-triflyl phosphoramide **HA6** are evidently capable of inducing relatively powerful conformational preferences in helical foldamers, but higher order complexes that diminish the h.e. are evidently possible. These competing interactions may arise from multiple hydrogen bonds to the NH$_3^+$ group in the protonated binding site **B2H$^+$**, disrupting the stoichiometric acid−base interaction **HA4↔F2**. This information prompted us to investigate alternative basic binding sites, and especially N-terminal pyridyl substituents **B3−B6** (Figure 1): such motifs can accept or (when protonated) donate only one hydrogen bond.

Foldamers **F3−6** were constructed containing the pyridine-carboxamide and pyridylacetamide binding sites **B3−6**, along with the two methylated pyridinium sites **B5Me$^+$** and **B6Me$^+$** that can ion-pair but not hydrogen bond. The $\Delta\delta$ values induced by acids **HA1−6** and anions **A7$^-$** and **A8$^-$** were measured in CDCl$_3$ (plus 28% MeOH for **A7$^-$** and **A8$^-$**) using the protocol described above (Table 1, entries 3−8).

In the case of **F3**, the phosphoric acids (**HA2**, **HA4**, **HA5**) and phosphoramide **HA6** induced a weak conformational preference (entry 3). Moving to the more flexible but more basic N-terminal 2- and 3-pyridinylacetyl motifs **B4** and **B6** led to higher levels of conformational induction from all three groups of acid ligands. More specifically, **HA4**, **HA1**, and **HA6** resulted in three distinct, decreasing chemical shift separations in N-terminal 2-pyridylacetyl foldamer **F4** (entry 4). A similar trend, with similar values for the induced helical excess, was observed with the longer oligomer **F4'** (entry 5). By contrast, conformational preferences in the N-terminal 3-pyridyl foldamer **F6** were reduced, except with **HA6** (entry 6). As a control experiment, **HA4**, **HA1**, and **HA6** were added to nonbasic foldamer **F7** (entry 9). Zero or very low induced screw-sense preferences were measured, confirming that any control arising from the chiral ligands occurs almost entirely from interactions at the N-terminal binding site.

Mixing chiral anions **A7$^-$** and **A8$^-$** with the methylated foldamers **F5Me$^+$** and **F6Me$^+$** induced some detectable conformational preferences, even in the presence of methanol, showing that ion pairing alone may be sufficient to transfer chiral information from the ligand to the foldamer, but the level of control was low (entries 7, 8). (The conformational

preferences in these cationic foldamers were quantified using a different set of ^{19}F-containing NMR reporters: see the SI for details.[69])

Nature of the Ligand-Binding Site Interaction. Having identified the 2-pyridylacetamide motif **B4** as a strong candidate in the search for a versatile and effective binding site for the development of a multicomponent signaling system, we next studied the stability of the ligand-foldamer pairs **HA1↔F4**, **HA4↔F4**, and **HA6↔F4** with respect to excess ligand and concentration. Varying the ratio **HA1:F4** (Figure 2) gave a
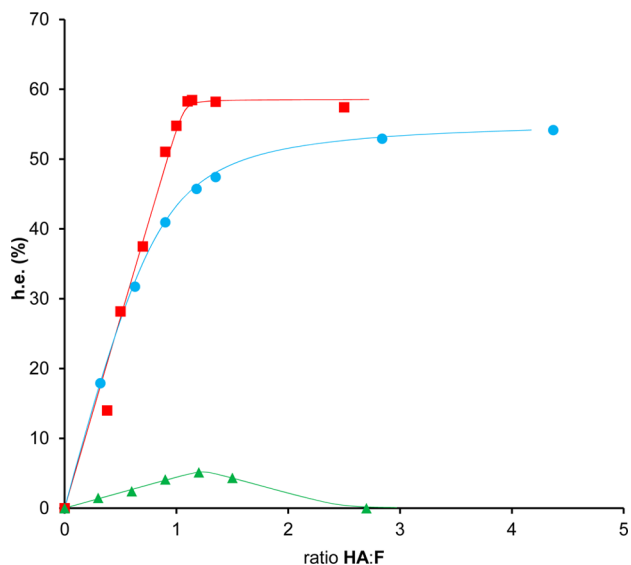

Figure 2. Conformational preference of foldamer **F4** (h.e.) at different ratios of **HA:F** in CDCl$_3$ at 296 K: 8.8 < [**F4**] < 10.0 mM for titration experiment with **HA1**; [**F4**] = 10.0 mM for titration experiments with **HA4** and **HA6**; blue ●, experimental data for **HA1**; red ■, experimental data for **HA4**; green ▲, experimental data for **HA6**. Curve fits shown for a 1:1 binding model using the program DynaFit: $K = 10^3$ M^{-1} (blue —), $K = 10^5$ M^{-1} (red —); Curve fit shown for a 2:1 binding model using the program DynaFit: $K = 10^7$ M^{-1} and $K' = 10^4$ M^{-1} (green —).

maximum induced helical excess of 55% for a ratio **HA1:F4** >3:1. A similar trend was observed for **HA4↔F4** with a maximum value around 59% h.e. for a ratio **HA4:F4** >1:1. In the case of **HA6↔F4**, the maximum conformational induction (around 6% h.e.) was obtained with a ratio **HA6:F4** = 1.2:1. In this case only, the $\Delta\delta$ value dropped in the presence of an excess of **HA6**, falling to 0 in the presence of 2.7 equiv of the ligand.

The change of h.e. upon binding of **HA1** and **HA4** to **F4** was fitted using a 1:1 binding model (see the SI). For **HA1**, a good fit to the data was found for a binding constant of $K = (1 \pm 0.3) \times 10^3$ M^{-1}, while for **HA4** the binding constant was found to be >10^5 M^{-1}. This large difference in binding affinity (by a factor of >10^2) was critical in allowing the development of complex systems capable of confomational switching. For **HA6**, the variation of h.e. on binding was fitted using a 2:1 binding model, which gave a good fit to the data with $K = 10^7$ M^{-1} and $K' = 10^4$ M^{-1} (see the SI).

Conformational induction in the **HA4↔F4** pair was remarkably concentration-independent: the induced helical excess was constant for [**F4**] ranging from 10 mM to 0.1 mM (ratio **HA:F** fixed at 1.2:1, Figure 3). In **HA6↔F4**, the conformational preference was likewise almost constant down
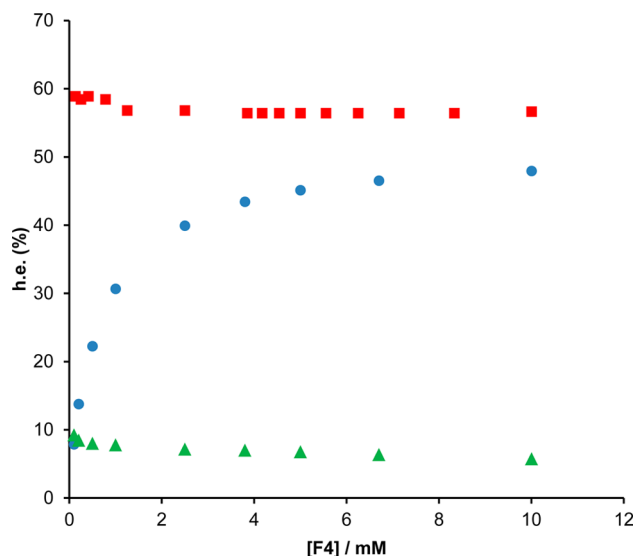

Figure 3. Conformational preference of foldamer **F4** (h.e.) at different concentrations of **F4** in CDCl$_3$ at 296 K with a fixed ratio **HA:F4**: blue ●, experimental data for **HA1:F4** = 1.5:1; red ■, experimental data for **HA4:F4** = 1.2:1; and green ▲, experimental data for **HA6:F4** = 1.2:1.

to 0.1 mM. In the less strongly bound pair **HA1↔F4**, h.e. varied little between 5 and 10 mM, but fell markedly at lower concentrations. These results also give a qualitative indication of the strength of binding in the **HA↔F4** pairs, with **HA6↔F4** ≥ **HA4↔F4** > **HA1↔F4**. The conformational effect of all three ligands was much weaker in the presence of a protic solvent: for example, addition of 2% MeOH to the solution in CDCl$_3$ induced a significant drop in the value of $\Delta\delta$ for the **HA4↔F4** interaction (SI Figure S56).

The nature of the interaction between the ligands and the binding site of **F4**[62,70−72] was examined by following the change in ^{13}C and ^{1}H NMR spectra as **HA1**, **HA4**, or **HA6** were titrated into a solution of **F4** in CDCl$_3$ at 296 K (SI Figures S35−37, S39−41, and S43−45). Addition of either **HA1**, **HA4**, or **HA6** led to gradual migration of ^{1}H NMR signals of the pyridine binding site to new positions, with the change in chemical shift being much more significant for **HA4** or **HA6** than for **HA1**. During the titration with **HA1**, none of the four proton signals from the pyridyl ring migrated by more than 0.13 ppm, though two of the NH protons of the foldamer chain exhibited a downfield shift. By contrast, during the titrations with **HA4** and **HA6**, the protons in the 4- and 5-positions of the pyridine ring migrated downfield by 0.5−0.6 and 0.25 ppm respectively, while the proton in the 6-position migrated upfield by 0.6−0.7 ppm. In addition, the migration of the peaks to new positions is complete after the addition of 1.0 equiv for **HA4**, while with **HA6**, the addition of more than one equivalent of the acid leads to further changes in the ^{1}H NMR spectrum that could be explained by protonation of other, less basic sites within **F4** by this extremely strong acid. Finally, similar experiments with HCl led to downfield shifts (of 0.1− 0.7 ppm) for all pyridyl protons (SI Figure S57).

In nonpolar solvents, neutral bases such as amines and pyridines are markedly less basic than anionic species, such as carboxylates, due to poor stabilization of charged species.[73] Acid−base interactions in chloroform are likely to start from hydrogen bonding, which under certain conditions can evolve into proton transfer from acid to base and, infrequently, dissociation of the resulting hydrogen-bonded ion pair. The

extent of proton transfer in a hydrogen-bonded complex is dictated mainly by the difference of basicities of the acid anion and base in the given medium.[74] The titration results suggest that the interaction of **F4** with the stronger acids **HA4** and **HA6** leads to extensive proton transfer from acid to the pyridine binding site and formation of a strong ionic hydrogen bond (a tightly hydrogen-bonded ion pair). **HA1**, by contrast, is insufficiently acidic to allow proton transfer to the pyridine site, yet still forms a hydrogen-bonded complex with **F4** that is additionally stabilized by interaction with two of the NH protons at the N terminus of the foldamer chain. Estimates of the relative pK_a values of **HA1**, **HA4**, and **HA6** in 1,2-dichloroethane (DCE) are shown in Table 2 along with the

Table 2. Estimated and Reported pK_a Values of Acids in 1,2-Dichloroethane Relative to 2,4,6-Trinitrophenol (see SI for Details)

acid	base	relative pK_a (DCE)
AcOH	AcO$^-$	15.5[a]
HA1	**A1$^-$**	12[b]
HA4	**A4$^-$**	3[c]
HCl	Cl$^-$	−0.4[d]
HA6	**A6$^-$**	−5.2[c]

[a]Calculated value from ref 73. [b]estimated using COSMO-RS calculations. [c]estimated using experimental pK_a values in acetonitrile. [d]experimental value from ref 75.

reported so-called "ion-pair"[75] pK_a values for AcOH and HCl in DCE (all pK_a values are relative to 2,4,6-trinitrophenol). 1,2-Dichloroethane was used as a model for chloroform due to scarcity of reported acidity data in the latter, and the similarity between the properties of these two solvents was confirmed using COSMO-RS[76] calculations. The pK_a estimates were calculated using linear regressions between pK_a values in DCE and acetonitrile (**HA4**, **HA6**), and between pK_a values in DCE and acid dissociation energies by COSMO-RS (**HA1**) (for further details, see SI). Pyridine is known to be remarkably less basic than acetate in aprotic or low-polarity solvents (e.g., ΔpK_a is ~9 in DMSO[77] and ~11 in acetonitrile[78,79]) and this basicity gap tends to increase with decreasing solvent polarity. Thus, we expect **F4H$^+$** to have a pK_a close to, but lower than, that of **HA4**. This is also in agreement with the observed strong binding between **HA4** and **F4**, as structures with proton affinities (pK_a values) of similar magnitude tend to produce the strongest hydrogen bonds.[74]

Importantly, screw sense induction by **HA1** and **HA4** (Figure 4b,f) was dramatically reduced or turned off when the pH[80] was raised by addition of ammonia (1 equiv relative to **HA**) to the mixture (Figure 4c,g). In the case of **HA1**, this additional equivalent of NH$_3$ presumably disrupts the **HA1**↔**F4** pair by forming a stronger hydrogen bonded complex **HA1**↔NH$_3$, because ammonia is more basic than pyridine in all solvents where data are available and thus most probably also in chloroform. For **HA4**, the disruption of the **HA4**↔**F4** pair may be rationalized by deprotonation of the partially or fully formed pyridinium ion **F4H$^+$**, replacing the interaction of **A4$^-$** and **F4H$^+$** by a tight ion pair between **A4$^-$** and NH$_4^+$. Addition of an equivalent of HCl led to precipitation of NH$_4$Cl, restoring the conformational induction in both cases. The lower level of control in the case of **HA1** possibly results from competing interactions with Cl$^-$ ions remaining in solution (Figure 4d and 4h).
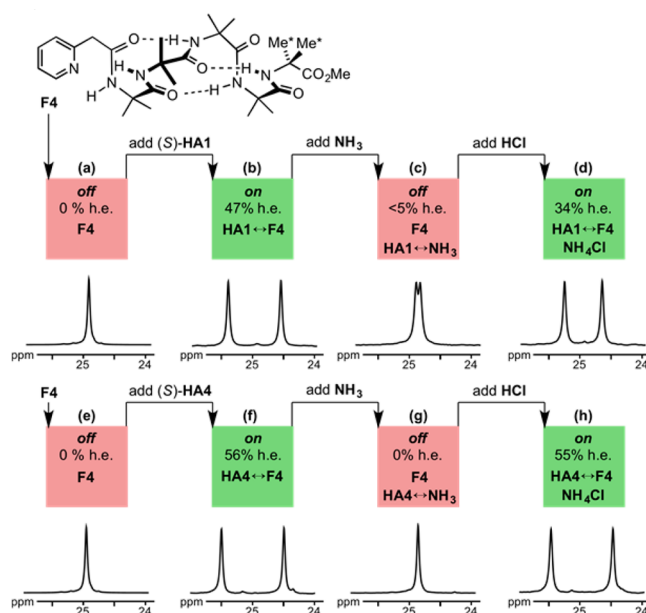

Figure 4. Switching induction on or off by use of acid or base. Portions of the ^{13}C spectra in CDCl$_3$ at 296 K of **F4** in the presence of ligand **HA**, **HA**+NH$_3$, and **HA**+NH$_3$+HCl.

Screw-sense inversion of Aib oligomers occurs on a submillisecond time scale at room temperature.[81] In other words, room temperature ^{13}C (ref 67) and ^{1}H (refs 58,82) NMR spectra lie in the fast exchange regime with respect to screw sense inversion. The peak shapes in the ^{1}H NMR spectra resulting from titrations of **F4** with **HA1** or **HA6** remain constant and more or less sharp throughout the experiment (SI Figures. S35, S36, and S43−44). This result is consistent with rapid exchange (on the NMR time scale) of **F4** not only between screw-sense conformers, but also between bound and unbound states when a substoichiometric quantity of either ligand is present. By contrast, addition of substoichiometric amounts of **HA4** to **F4** gives rise to exchange broadening in the ^{1}H NMR spectrum, with peaks sharpening again as more of the ligand is added (SI Figures S39 and S40). This result suggests slower exchange of **F4** between bound and unbound states, with the coalescence temperature for this exchange process lying close to ambient temperature.

Related behavior was evident in the ^{13}C NMR spectra (SI Figures S37, S41, and S45). With **HA1**, fast exchange between bound and unbound **F4** led to the separation between the peaks arising from the two ^{13}C labels increasing successively with additional quantities of **HA1** to reach a maximum of 959 ppb, corresponding to 54% h.e. Evidence for fast exchange between bound and unbound states was further provided by variable temperature ^{13}C and ^{1}H NMR experiments of a mixture of **F4** and 0.5 equiv **HA1**. The ^{13}C NMR spectrum of this mixture showed just one pair of sharp signals above 293 K that start to undergo decoalescence on lowering the temperature to 235 K (SI Figure S65). With **HA6**, similar incremental increases in peak separation were seen, but when more than one equivalent of acid was added, the Δδ value dropped to 0 ppb and the ^{13}C label signal migrated to a new position, presumably due to protonation of the peptide chain.

Behavior in the ^{13}C NMR spectrum during titration of **F4** with **HA4** was different, showing broadened signals characteristic of spectra in the intermediate exchange regime even at

room temperature. Variable temperature ^{13}C and ^{1}H NMR experiment of a mixture of 0.5 equiv **HA4** with **F4** (SI Figure S66) were consistent with a mixture of bound (a pair of signals in the ^{13}C NMR) and unbound (a single signal) states that are exchange-broadened at all temperatures between 235 and 313 K and that undergo coalescence at around 270 K. At 235 K, the singlet arising from the unbound state is just above coalescence, behavior consistent with the slowing of screw sense inversion to a time scale slightly faster than that of ligand binding.

Line shape simulations of the ^{13}C NMR spectra obtained during the titration of **F4** with **HA4** and of the VT ^{13}C NMR spectra obtained from the mixture **F4** with 0.5 equiv **HA4** (SI Figure S68) lend further support to our interpretation of these results in terms of exchange between bound and unbound states, and between left- and right-handed screw-sense, on a time scale of 10^{-5} - 10^{-6} s at 295 K (see the SI).

Competition between Ligands: A Three-Component System. At this stage of the study, it was clear that the 2-pyridylacetyl motif **B4** was capable of sustaining stable 1:1 interactions through hydrogen bonding and/or ion pairing with a range of chiral acids, with [**F**] from 10 to 7 mM or less and **HA1:F**, **HA4:F**, and **HA6:F** ratios from 1:1 to at least 1.5:1. We now needed to set up ligand exchange experiments between competing foldamer-ligand pairs **HAx↔F** vs **HAy↔F**. In order to establish which of the alternative pairs predominated, we chose systems in which competing ligands would each induce an opposite absolute screw sense in the foldamer. Absolute screw-sense preference in **HA↔F** pairs was determined using labeled foldamer **F4*** in which the C-terminal (R)-Aib*OMe residue is asymmetrically enriched in ^{13}C, with 75% ^{13}C in the pro-R Me group and 25% in the pro-S.[83] As a result, the major ^{13}C NMR signal appears downfield of the minor signal when the residue finds itself terminating a P-helix and upfield of the minor signal in an M-helix, allowing ^{13}C NMR to report on both the relative and absolute sense of conformational induction in the foldamer.[17,24,82] Preliminary experiments with **F4***, mixing with either (S)-**HA1**, (S)-**HA4** or (S)-**HA6**, showed that (S)-**HA1** and (S)-**HA4** induced a right-handed (P) screw sense while (S)-**HA6** induced (more weakly) a left-handed (M) screw sense (Figure 5a-c).

Now the scene was set for a competition experiment[70] between two ligands. (S)-**HA1** (1.5 equiv) was added to a solution of **F4*** (1.0 equiv) in CDCl$_3$ to induce P screw sense (Figure 6a,b) with the anisochronicity +904 ppb characteristic of the ca. 50% h.e. induced in the **HA1↔F4** pair (cf. Table 1, entry 4). On addition of the stronger acid (R)-**HA4** (1.5 equiv) to the mixture (Figure 6c), the major signal in the ^{13}C NMR spectrum moved upfield of the minor, indicating a switch in the screw sense preference of **F4*** from P to M.[27,84] The anisochronicity of the signals also increased in magnitude to −945 ppb, suggesting almost exclusive formation of a paired (R)-**HA4↔F4*** ligand-foldamer complex (Table 1, entry 4). Evidently, **HA4** can completely displace **HA1** from the pyridyl binding site, a result that is most readily understood as a consequence of the tighter pairing between the foldamer **F4*** and the stronger acid **HA4**.[62] In the absence of detailed knowledge about the extent of proton transfer in the acid−base pairs in this and subsequent studies, foldamer **F4*** is represented by a neutral pyridine ring irrespective of its probable protonation state: it may be assumed that this pyridine pairs with the most acidic species available, by a mechanism that we leave undefined diagrammatically.
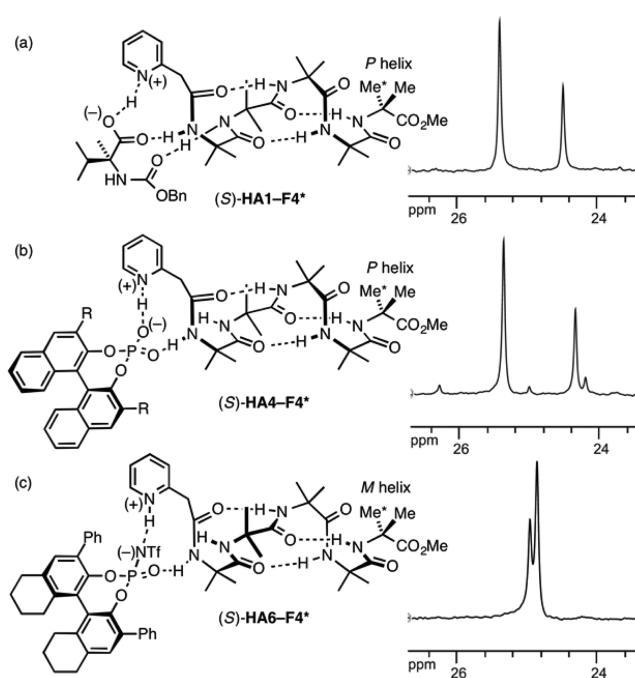

Figure 5. Portions of the ^{13}C spectra in CDCl$_3$ at 296 K of **F4*** showing absolute screw sense induced by (a) (S)-**HA1** [P], (b) (S)-**HA4** [P], and (c) (S)-**HA6** [M]. R = 2,4,6-triisopropylphenyl.

We reasoned that the interaction with, and hence the influence of, the carboxylic acid **HA1** would be restored by the addition of a base stronger than **F4*** in CDCl$_3$. Addition of ammonia (1.5 equiv) indeed induced a screw sense inversion back from M to P (Figure 6d). Presumably, the allocation of the proton available from **HA4** to NH$_3$ generates an ion pair NH$_4^+$**A4**$^-$ that allows the neutral, acidic **HA1** and the neutral, basic **F4*** to reform a screw-sense inducing **HA1↔F4*** interaction. The reduced anisochronicity of +423 ppb does however suggest some interference in this hydrogen-bonded interaction from the other acidic and basic species in solution.

Given that the relative dominance of competing ligands **HA1** or **HA4** may evidently be decided by the availability of protons, we reasoned that screw sense in **F4*** should be switchable simply by addition either of base (to favor the P helical pairing **HA1↔F4***) or of acid (to favor the M helical pairing **HA4↔F4***). Adding HCl (1.5 equiv) to the previous mixture of **HA1**, **HA4**, **F4*** and NH$_3$ led to a switch in screw sense from P back to M (Figure 6e) as the **HA4↔F4*** interaction is restored by the additional proton now made available. This change was accompanied by a white precipitate, attributed to the formation of NH$_4$Cl. The protonation was reversible, and adding again NH$_3$ (1.5 equiv) switched back on the **HA1↔F4*** interaction and inverted again **F4***'s screw sense from M to P (Figure 6f). After each switching cycle, the anisochronicity of ca. −950 ppb induced in **F4*** by the stronger acid **HA4** was resilient in the presence of the other species in the mixture, while that induced by **HA1** continued to decline, despite the apparent removal of NH$_4$Cl from solution by precipitation.

Having demonstrated reversible switching between the two states M (in **HA4↔F4***) and P (in **HA1↔F4***), we added another 1.5 equiv of NH$_3$. As a result, **F4*** entered a third conformational state in which it recorded no screw-sense preference (Figure 6g). Presumably the stronger base NH$_3$ now displaces the weaker **F4*** from the **HA1↔F4*** pair, leaving **F4*** unable to interact with **HA1**. This conformationally racemic ±

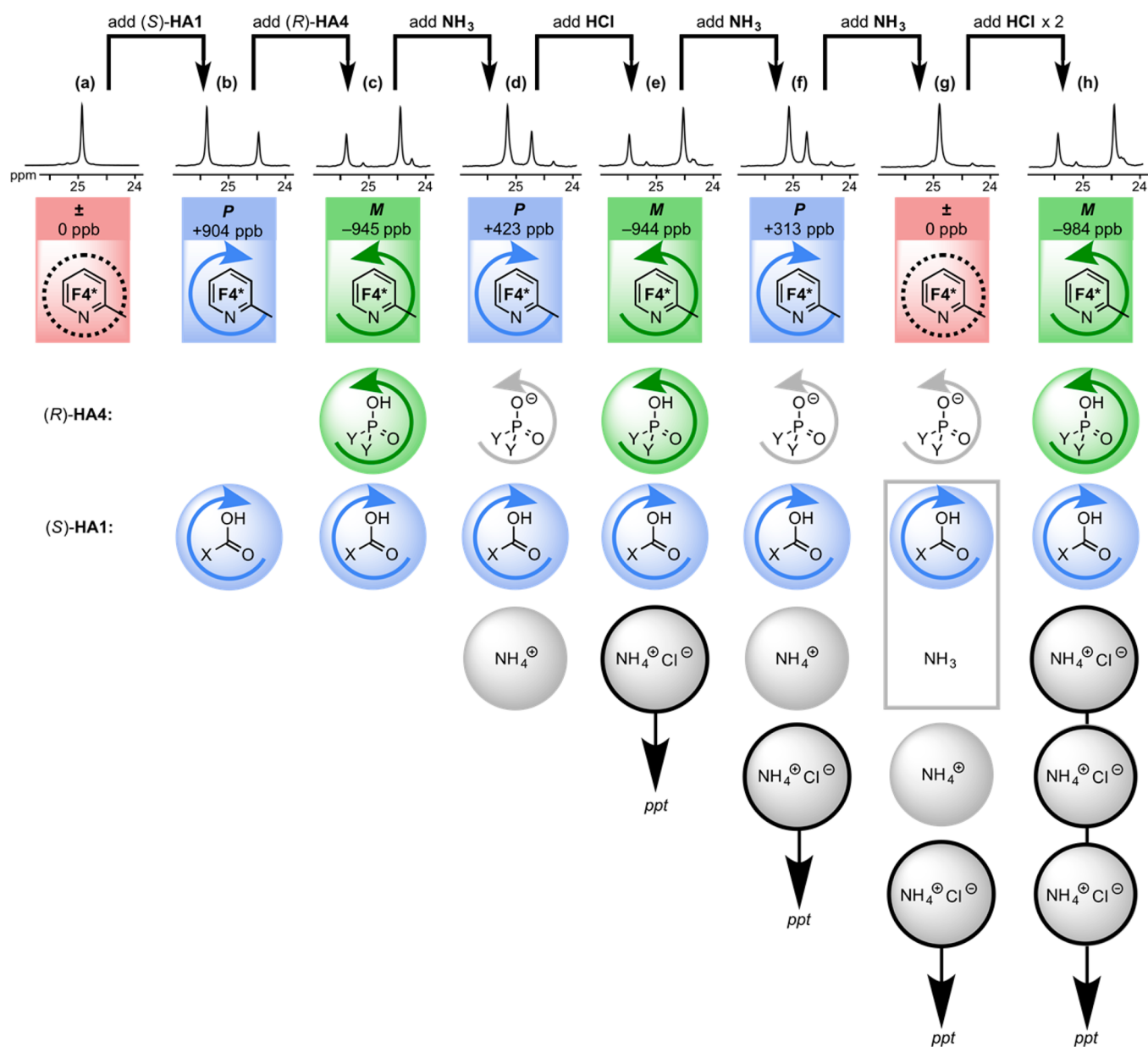**Figure 6.** Conformational switching of foldamer **F4*** with competing chiral ligands. [**F4***] = 10 mM, CDCl$_3$, 296 K; all subsequent additions are of 1.5 equiv relative to **F4***. Portions of the ^{13}C NMR spectra of the mixtures containing the labeled signals of **F4*** are shown, with anisochronicity $\Delta\delta$ reported as the difference in chemical shift between the major and minor labeled signals of **F4***, $\delta^{maj} - \delta^{min}$, measured in ppb. Protonated species available for interaction with the **F4*** binding site (represented by the pyridine in the colored rectangle) are indicated by blue/green (for chiral species) or gray (for achiral species) disks, and acids **HA** are stacked in order of pK_a in CDCl$_3$. The number of protons available is represented by the number of discs, building up from the bottom of the stack. Proposed conformation-inducing interactions with **F4*** (whether these are hydrogen-bonded or ion-paired is left undefined) are coded by matched colors: blue indicates induction of a P screw-sense; green indicates induction of an M screw-sense; red indicates no screw-sense induction. The most significant interaction is assumed to be between **F4*** and the top (typically the most acidic) protonated species in each multiply protonated stack.

resting state could be "reactivated" with HCl: adding two portions (3.0 equiv) to the previous solution reprotonated the excess ammonia and reinstated the **HA4**↔**F4*** pair, restoring a powerful ($\Delta\delta = -984$ ppb) M screw-sense preference (Figure 6h).

Overall then, the three-component chemical system comprising **F4***, **HA1** and **HA4** may be switched at will between three alternative conformational states (in this case $\pm \rightarrow P \rightarrow M \rightarrow P \rightarrow M \rightarrow P \rightarrow \pm \rightarrow M$) by successive additions and subtractions of protons, forcing the pH-dependent[85] selective exchange of ligands at the pyridylacetyl binding site.

Switching in Four-Component Systems. Encouraged by the responsiveness of this three-component system, we investigated the potential for acidity-driven conformational switching in a four-component system composed of **F4***, (R)-**HA1**, (S)-**HA4**, and (S)-**HA6**. Starting with a solution of **F4*** (1.0 equiv) in CDCl$_3$ (Figure 7a) we added (R)-**HA1** (1.5 equiv), inducing an M screw sense in **F4*** (Figure 7b), followed by (R)-**HA4** (1.5 equiv), inverting the screw-sense of **F4*** from M to P (Figure 7c). Now, addition of (S)-N-triflyl phosphoramide **HA6** (1.5 equiv) to this mixture induces a second helical inversion from P back to M (Figure 7d), with a
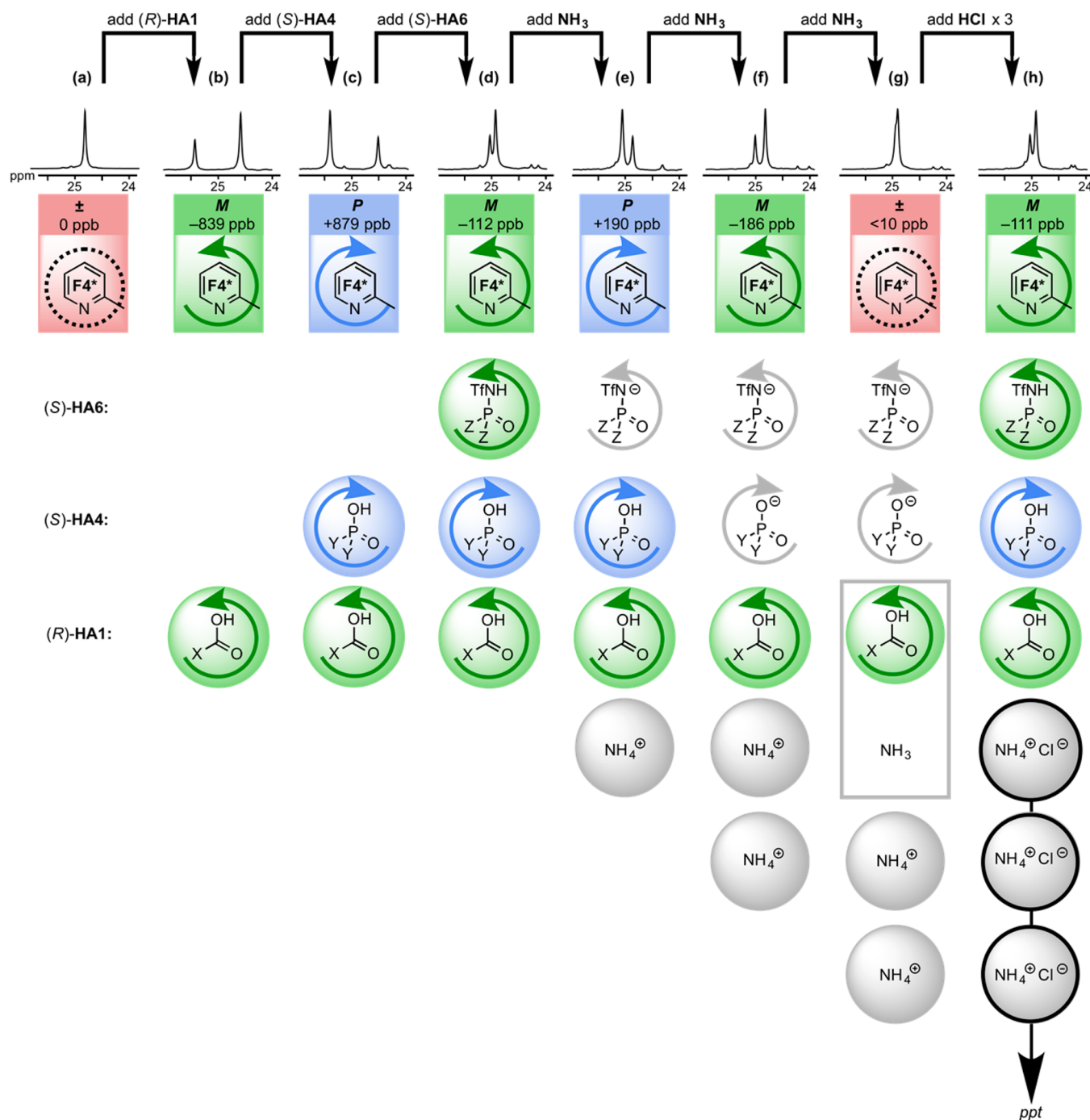
Figure 7. Conformational switching of foldamer **F4*** with three competing chiral ligands. [**F4***] = 10 mM, CDCl$_3$, 296 K; all subsequent additions are of 1.5 equiv relative to **F4***. Portions of the ^{13}C NMR spectra of the mixtures containing the labeled signals of **F4*** are shown, with anisochronicity $\Delta\delta$ reported as the difference in chemical shift between the major and minor labeled signals of **F4***, $\delta^{maj} - \delta^{min}$, measured in ppb. Protonated species available for interaction with the **F4*** binding site (represented by the pyridine in the colored rectangle) are indicated by blue/green (for chiral species) or gray (for achiral species) disks, and acids **HA** are stacked in order of pK_a. The number of protons available is represented by the number of discs, building up from the bottom of the stack. Proposed conformation-inducing interactions with **F4*** (whether these are hydrogen-bonded or ion-paired is left undefined) are coded by matched colors: blue indicates induction of a *P* screw-sense; green indicates induction of an *M* screw-sense; red indicates no screw-sense induction. The most significant interaction is assumed to be between **F4*** and the top (typically the most acidic) protonated species in each multiply protonated stack. 7(g) is an exception: **A1**$^-$ is probably protonated rather than NH$_3$, but the lack of screw sense preference in **F4*** suggests interaction preferentially with an NH$_4^+$ ion.

value of $\Delta\delta = -112$ ppb. We presume that **HA6** takes control of the conformation of the foldamer **F4*** by protonating the **HA4**↔**F4*** pairing of the weaker acid **HA4** and inducing a conformational preference characteristic of the new (probably

largely ion-paired[62]) **HA6**↔**F4*** interaction (cf. Table 1, entry 4).

Next, 4.5 equiv of ammonia was added in 1.5 equiv portions to the four-component system. The screw sense of **F4*** switched from *M* to *P* (Figure 7e) as the first 1.5 equiv was
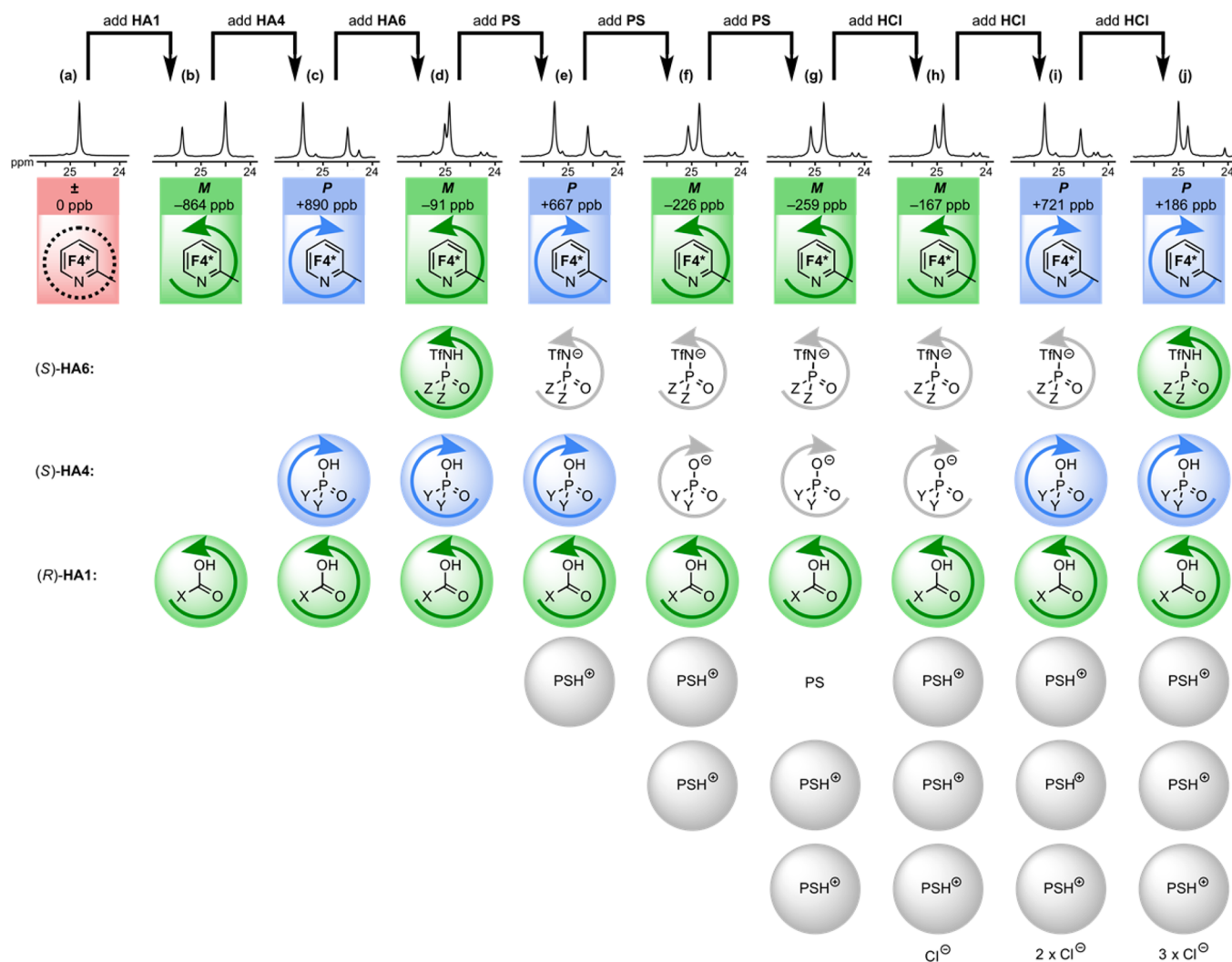
Figure 8. Conformational switching of foldamer **F4*** with three competing chiral ligands in a single phase. PS = proton sponge. [**F4***] = 10 mM, CDCl₃, 296 K; all subsequent additions are of 1.5 equiv relative to **F4***. Portions of the ^{13}C NMR spectra of the mixtures containing the labeled signals of **F4*** are shown, with anisochronicity $\Delta\delta$ reported as the difference in chemical shift between the major and minor labeled signals of **F4***, $\delta^{maj} - \delta^{min}$, measured in ppb. Protonated species available for interaction with the **F4*** binding site (represented by the pyridine in the colored rectangle) are indicated by blue/green (for chiral species) or gray (for achiral species) disks, and acids **HA** are stacked in order of pK_a. The number of protons available is represented by the number of discs, building up from the bottom of the stack. Proposed conformation-inducing interactions with **F4*** (whether these are hydrogen-bonded or ion-paired is left undefined) are coded by matched colors: blue indicates induction of a P screw-sense; green indicates induction of an M screw-sense; and red indicates no screw-sense induction. The most significant interaction is assumed to be between **F4*** and the top (typically the most acidic) protonated species in each multiply protonated stack.

added, then back to M with the second 1.5 equiv (Figure 7f), and then to the ± state with the third 1.5 equiv (Figure 7g). Neutralizing the 4.5 equiv ammonia with 4.5 equiv HCl took the system back to the P state (Figure 7h) corresponding to the **HA6**↔**F4*** interaction, with magnitude of conformational control similar to that observed originally (cf. Figure 7d,h).

The cyclic switching of screw sense with successive additions of ammonia can be accounted for by ammonia first disrupting the most acidic triflamide pairing **HA6**↔**F4*** (Figure 7e) then the phosphoric acid−pyridine pairing **HA4**↔**F4*** (Figure 7f) and finally the least acidic carboxylic acid−pyridine pairing **HA1**↔**F4*** (Figure 7g). In other words, the three additions of ammonia each provide a favorable, basic destination for the three protons initially supplied to the system by the three acids, leaving the foldamer **F4*** to choose a partner from the acid species that remain after each addition. In Figure 7e the selective interaction of **F4*** with **HA4** rather than **HA1** may be

driven principally by the relative acidity of **HA4**, while in Figure 7f an additional factor in the choice of **HA1** over the probably more acidic NH₄⁺ may be the involvement of NH₄⁺ in stronger ion pairing interactions with **A6**⁻ and **A4**⁻. As ammonium counterions build up in solution, the level of conformational induction is reduced, presumably because they compete as (achiral, screw-sense neutral) acid ligands for **F4***. The final addition of NH₃ (Figure 7g) offers even the weakest acid **HA1** a more basic partner than **F4***, so **F4*** is left unpartnered in an achiral environment. Final addition of 4.5 equiv HCl precipitated the added base from solution as ammonium chloride, and completed the cycle of switching of **F4*** from ± → M → P → M → P → M → ± → M and restores fully the degree and sense of conformational control supplied by the triflamide **HA6**.

Aiming to avoid the deteriorating conformational control that appears to result from the accumulation of hydrogen-bond

donating ammonium ions, we repeated the acid−base switching experiment with proton sponge[86] (PS, 1,8-bis(dimethylamino)-naphthalene), selected as an alternative base to NH$_3$ that will sequester the accepted proton with an internal hydrogen bond. The results are shown in Figure 8, where stages a−d match the switching process of Figure 7a−d. Addition of PS (1.5 equiv) to the four component system **F4***+**HA1**+**HA4**+**HA6** of Figure 8d induced a conformational switch from *M* to *P* (Figure 8e) as observed with ammonia (Figure 7e), but with much greater retention of conformational control [$\Delta\delta$ = +667 ppb in the presence of PSH$^+$ (Figure 8e), compared with +890 ppb in the absence of cations (Figure 8c) and only +190 ppb in the presence of NH$_4^+$ (Figure 7e)]. The second addition of PS (1.5 equiv) switched screw-sense from *P* to *M* (Figure 8f) but this time with only marginally greater conformational control than with NH$_3$ (Figure 7f). Unlike with NH$_3$, the third addition of PS (1.5 equiv) did not result in the system switching to the resting ± state: an induced *M* screw sense was still observed (Figure 8g). Working back up the acidity scale, a first addition of HCl (1.5 equiv) had no influence on the system, which remained *M* (Figure 8h), and a second addition of HCl (1.5 equiv) induced a switch from *M* to *P* with good recovery of the conformational control typical of **HA4**↔**F4*** . However, a third addition of HCl (1.5 equiv) did not result in the switch from *P* to *M* as seen with ammonia as base (Figure 7h)—instead **F4*** remained in the *P* screw-sense, but with a reduced magnitude of conformational control extent (Figure 8i).

The inability of PS to disrupt the **HA1**↔**F4*** interaction (Figure 8g) suggests that while PS and NH$_3$ are both insufficiently basic to deprotonate carboxylic acid **HA1**, NH$_3$ hydrogen bonds strongly to **HA1**, disrupting its interaction with **F4*** (Figure 7g). In contrast, steric hindrance at the basic site in PS may prevent strong hydrogen-bonding to **HA1**,[87] leaving the **HA1**↔**F4*** interaction intact.

The lack of recovery of *M* screw sense on acidification to the final **F4***+**HA1**+**HA4**+**HA6**+(3 × PS)+(3 × HCl) mixture (Figure 8i) seems likely to arise from the contrasting behavior of NH$_4$Cl (which precipitates from chloroform) and PS·HCl (which remains in solution). In this final mixture, the system has six protons to distribute between seven bases, so the mixture presumably contains 3 × PSH$^+$, HF**4**$^+$, **HA1**, **HA4**, **A6**$^-$, and three Cl$^-$ ions. Before the final acidification step, the conformation-controlling interaction is that between the strongest base **F4*** and the strongest acid **HA4** (Figure 8i). We expected addition of HCl to protonate **A6**$^-$, hence disrupting **HA4**↔**F4*** and allowing **HA6**↔**F4*** to form, an opportunity which it evidently nonetheless does not take. This observation can be rationalized by assuming that the weak *M* preference of the **HA6**↔**F4*** ion pair (seen in Table 1 entry 4, Figure 7d and Figure 8d) is sensitive to disruption by the high concentration (4.5 equiv relative to **F4***) of other ionic material in solution. More strongly hydrogen-bonded, rather than principally ion-paired, interactions seem less susceptible to interference by the presence of dissolved salts (cf. Figure 8c,e,g; Figure 8f,h).

CONCLUSIONS

Selecting interactions among the many possible within a multicomponent chemical mixture leads a peptidomimetic foldamer to adopt a specific conformational preference, which may be quantified by ^{13}C NMR. Alternative permutations of mutual interactions among the components of the system may be activated by controlling the protonation state of the system.

In response to changes in acidity, the foldamer chooses, from a suite of ligands of graded basicity, a partner whose binding is identifiable by the specific, ligand-dependent conformational preference it induces in the foldamer. Competing ligands are simultaneously rendered ineffective by stronger silencing interactions with alternative acids or bases, but each may nonetheless be restored to activity by adding or subtracting protons. By choosing chiral ligands of appropriate configuration, pH changes can be used to switch the foldamer reversibly between left- and right-handed conformations[84,88] with conformational preferences characteristic of the ligands employed. The chemical system thus behaves as a simple proton-counting device.[25,26,89−91] It can also be viewed as an acidity-sensitive conformational indicator,[92−103] whose analogue spectroscopic output (measurable by the relative positions of two peaks in the ^{13}C NMR spectrum) is dictated by a conformational preference that is itself a function of the number of protons available in the mixture. Future work will seek to develop more complex synthetic networks of conformationally responsive interacting molecules.

■ ASSOCIATED CONTENT

ⓈSupporting Information
Characterization data for all new compounds. Full details of titration and NMR experiments. The Supporting Information is available free of charge on the ACS Publications website at DOI: 10.1021/jacs.5b03284.

■ AUTHOR INFORMATION

Corresponding Author
*clayden@man.ac.uk
Notes
The authors declare no competing financial interest.

■ ACKNOWLEDGMENTS

■ REFERENCES

(1) Lehn, J.-M. *Chem.—Eur. J.* **2000**, *6*, 2097−2102.
(2) Sarma, R. J.; Nitschke, J. R. *Angew. Chem., Int. Ed.* **2008**, *47*, 377−380.
(3) Thomas, S. W.; Chiechi, R. C.; LaFratta, C. N.; Webb, M. R.; Lee, A.; Wiley, B. J.; Zakin, M. R.; Walt, D. R.; Whitesides, G. M. *Proc. Natl. Acad. Sci. U. S. A.* **2009**, *106*, 9147−9150.
(4) Safont-Sempere, M. M.; Fernández, G.; Würthner, F. *Chem. Rev.* **2011**, *111*, 5784−5814.
(5) Milroy, L.-G.; Grossmann, T. N.; Hennig, S.; Brunsveld, L.; Ottmann, C. *Chem. Rev.* **2014**, *114*, 4695−4748.
(6) Grauer, A.; König, B. *Eur. J. Org. Chem.* **2009**, *2009*, 5099−5111.
(7) Ha, J.-H.; Loh, S. N. *Chem.—Eur. J.* **2012**, *18*, 7984−7999.
(8) Smith, C. A.; Ban, D.; Pratihar, S.; Giller, K.; Schwiegk, C.; de Groot, B. L.; Becker, S.; Griesinger, C.; Lee, D. *Angew. Chem., Int. Ed.* **2015**, *54*, 207−210.
(9) Nevola, L.; Giralt, E. *Chem. Commun.* **2015**, *51*, 3302−3315.
(10) Perutz, M. F. *Q. Rev. Biophys.* **1989**, *22*, 139−236.
(11) Shibayama, N.; Sugiyama, K.; Tame, J. R. H.; Park, S.-Y. *J. Am. Chem. Soc.* **2014**, *136*, 5097−5105.

(12) Yuan, Y.; Tam, M. F.; Simplaceanu, V.; Ho, C. *Chem. Rev.* **2015**, *115*, 1702−1724.

(13) Perutz, M. F. *Nature (London)* **1988**, *336*, 202−203.

(14) Dudev, T.; Lim, C. *Sci. Rep.* **2015**, *5*, 7864.

(15) Davis, R. B., Jr.; Lecomte, J. T. J. *Proteins* **2005**, *63*, 336−348.

(16) Krauss, R.; Koert, U. *Synlett* **2003**, 598−608.

(17) Solà, J.; Fletcher, S. P.; Castellanos, A.; Clayden, J. *Angew. Chem., Int. Ed.* **2010**, *49*, 6836−6839.

(18) Clayden, J.; Lund, A.; Vallverdu, L. S.; Helliwell, M. *Nature (London)* **2004**, *431*, 966−971.

(19) Clayden, J.; Vassiliou, N. *Org. Biomol. Chem.* **2006**, *4*, 2667−2678.

(20) Clayden, J. *Chem. Soc. Rev.* **2009**, *38*, 817−829.

(21) Gellman, S. H. *Acc. Chem. Res.* **1998**, *31*, 173−180.

(22) Hill, D. J.; Mio, M. J.; Prince, R. B.; Hughes, T. S.; Moore, J. S. *Chem. Rev.* **2001**, *101*, 3893−4012.

(23) Hecht, S.; Huc, I. *Foldamers: Structure, Properties and Applications*; Wiley-VCH: Weinheim, 2007.

(24) Brown, R. A.; Diemer, V.; Webb, S. J.; Clayden, J. *Nat. Chem.* **2013**, *5*, 853−860.

(25) Shigeno, M.; Kushida, Y.; Kobayashi, Y.; Yamaguchi, M. *Chem.—Eur. J.* **2014**, *20*, 12759−12762.

(26) Pischel, U. *Angew. Chem., Int. Ed. Engl.* **2007**, *46*, 4026−4040.

(27) Knipe, P. C.; Thompson, S.; Hamilton, A. D. *Chem. Sci.* **2015**, *6*, 1630−1639.

(28) Knipe, P. C.; Lingard, H.; Jones, I. M.; Thompson, S.; Hamilton, A. D. *Org. Biomol. Chem.* **2014**, *12*, 7937−7941.

(29) Mendez-Arroyo, J.; Barroso-Flores, J.; Lifschitz, A. M.; Sarjeant, A. A.; Stern, C. L.; Mirkin, C. A. *J. Am. Chem. Soc.* **2014**, *136*, 10340−10348.

(30) Sairenji, S.; Akine, S.; Nabeshima, T. *Tetrahedron Lett.* **2014**, *55*, 1987−1990.

(31) Suk, J.-M.; Naidu, V. R.; Liu, X.; Lah, M. S.; Jeong, K.-S. *J. Am. Chem. Soc.* **2011**, *133*, 13938−13941.

(32) Jones, I. M.; Hamilton, A. D. *Angew. Chem., Int. Ed.* **2011**, *50*, 4597−4600.

(33) Ulrich, S.; Lehn, J.-M. *J. Am. Chem. Soc.* **2009**, *131*, 5546−5559.

(34) Clayden, J.; Vallverdú, L.; Clayton, J.; Helliwell, M. *Chem. Commun.* **2008**, 561−563.

(35) Meudtner, R. M.; Hecht, S. *Angew. Chem., Int. Ed.* **2008**, *47*, 4926−4930.

(36) Nishimura, T.; Maeda, K.; Yashima, E. *Chirality* **2004**, *16*, S12−S22.

(37) Tamoto, R.; Daugey, N.; Buffeteau, T.; Kauffmann, B.; Takafuji, M.; Ihara, H.; Oda, R. *Chem. Commun.* **2015**, *51*, 3518−3521.

(38) Miyake, H.; Tsukube, H. *Chem. Soc. Rev.* **2012**, *41*, 6977−6991.

(39) Pijper, D.; Feringa, B. L. *Soft Matter* **2008**, *4*, 1349−1372.

(40) Yashima, E.; Maeda, K. *Macromolecules* **2008**, *41*, 3−12.

(41) Maeda, K.; Yashima, E. In *Supramolecular Chirality: Topics in Current Chemistry*; Springer-Verlag: Berlin/Heidelberg, 2006; Vol. 265, pp 47−88.

(42) Inai, Y.; Tagawa, K.; Takasu, A.; Hirabayashi, T.; Oshikawa, T.; Yamashita, M. *J. Am. Chem. Soc.* **2000**, *122*, 11731−11732.

(43) Inai, Y.; Ousaka, N.; Ookouchi, Y. *Biopolymers* **2006**, *82*, 471−481.

(44) Ousaka, N.; Inai, Y.; Okabe, T. *Biopolymers* **2006**, *83*, 337−351.

(45) Ousaka, N.; Inai, Y.; Kuroda, R. *J. Am. Chem. Soc.* **2008**, *130*, 12266−12267.

(46) Ousaka, N.; Inai, Y. *J. Org. Chem.* **2009**, *74*, 1429−1439.

(47) Inai, Y.; Ousaka, N.; Okabe, T. *J. Am. Chem. Soc.* **2003**, *125*, 8151−8162.

(48) Le Bailly, B. A. F.; Byrne, L.; Diemer, V.; Foroozandeh, M.; Morris, G. A.; Clayden, J. *Chem. Sci.* **2015**, *6*, 2313−2322.

(49) Toniolo, C.; Crisma, M.; Formaggio, F.; Peggion, C. *Biopolymers* **2001**, *60*, 396−419.

(50) Venkatraman, J.; Shankaramma, S. C.; Balaram, P. *Chem. Rev.* **2001**, *101*, 3131−3152.

(51) Toniolo, C.; Benedetti, E. *Trends Biochem. Sci.* **1991**, *16*, 350−353.

(52) Karle, I. L.; Balaram, P. *Biochemistry* **1990**, *29*, 6747−6756.

(53) Toniolo, C.; Bonora, G. M.; Barone, V.; Bavoso, A.; Benedetti, E.; Di Blasio, B.; Grimaldi, P.; Lelj, F.; Pavone, V.; Pedone, C. *Macromolecules* **1985**, *18*, 895−902.

(54) Prasad, B. V.; Balaram, P. *CRC Crit. Rev. Biochem.* **1984**, *16*, 307−348.

(55) Pengo, B.; Formaggio, F.; Crisma, M.; Toniolo, C.; Bonora, G. M.; Broxterman, Q. B.; Kamphuis, J.; Saviano, M.; Iacovino, R.; Rossi, F.; Benedetti, E. *J. Chem. Soc., Perkin Trans. 2* **1998**, 1651−1657.

(56) Clayden, J.; Castellanos, A.; Solà, J.; Morris, G. A. *Angew. Chem., Int. Ed.* **2009**, *48*, 5962−5965.

(57) Solà, J.; Helliwell, M.; Clayden, J. *J. Am. Chem. Soc.* **2010**, *132*, 4548−4549.

(58) De Poli, M.; Byrne, L.; Brown, R. A.; Solà, J.; Castellanos, A.; Boddaert, T.; Wechsel, R.; Beadle, J. D.; Clayden, J. *J. Org. Chem.* **2014**, *79*, 4659−4675.

(59) Byrne, L.; Solà, J.; Boddaert, T.; Marcelli, T.; Adams, R. W.; Morris, G. A.; Clayden, J. *Angew. Chem., Int. Ed.* **2014**, *53*, 151−155.

(60) Ousaka, N.; Takeyama, Y.; Iida, H.; Yashima, E. *Nat. Chem.* **2011**, *3*, 856−861.

(61) Ousaka, N.; Takeyama, Y.; Yashima, E. *Chem.—Eur. J.* **2013**, *19*, 4680−4685.

(62) Parmar, D.; Sugiono, E.; Raja, S.; Rueping, M. *Chem. Rev.* **2014**, *114*, 9047−9153.

(63) Lacour, J.; Ginglinger, C.; Grivet, C.; Bernardinelli, G. *Angew. Chem., Int. Ed. Engl.* **1997**, *36*, 608−610.

(64) Lacour, J.; Londez, A.; Goujon-Ginglinger, C.; Buss, V.; Bernardinelli, G. *Org. Lett.* **2000**, *2*, 4185−4188.

(65) Evans, N. H.; Beer, P. D. *Angew. Chem., Int. Ed.* **2014**, *53*, 11716−11754.

(66) Phipps, R. J.; Hamilton, G. L.; Toste, F. D. *Nat. Chem.* **2012**, *4*, 603−614.

(67) Solà, J.; Morris, G. A.; Clayden, J. *J. Am. Chem. Soc.* **2011**, *133*, 3712−3715.

(68) Pike, S. J.; Diemer, V.; Raftery, J.; Webb, S. J.; Clayden, J. *Chem.—Eur. J.* **2014**, *20*, 15981−15990.

(69) Pike, S. J.; De Poli, M.; Zawodny, W.; Raftery, J.; Webb, S. J.; Clayden, J. *Org. Biomol. Chem.* **2013**, *11*, 3168−3176.

(70) Kadam, S. A.; Martin, K.; Haav, K.; Toom, L.; Mayeux, C.; Pung, A.; Gale, P. A.; Hiscock, J. R.; Brooks, S. J.; Kirby, I. L.; Busschaert, N.; Leito, I. *Chem.—Eur. J.* **2015**, *21*, 5145−5160.

(71) Manabe, K.; Okamura, K.; Date, T.; Koga, K. *J. Am. Chem. Soc.* **2002**, *115*, 5324−5325.

(72) Fitzmaurice, R. J.; Kyne, G. M.; Douheret, D.; Kilburn, J. D. *J. Chem. Soc., Perkin Trans. 1* **2002**, 841−864.

(73) Raamat, E.; Kaupmees, K.; Ovsjannikov, G.; Trummal, A.; Kütt, A.; Saame, J.; Koppel, I.; Kaljurand, I.; Lipping, L.; Rodima, T.; Pihl, V.; Koppel, I. A.; Leito, I. *J. Phys. Org. Chem.* **2013**, *26*, 162−170.

(74) Gilli, P.; Gilli, G. *J. Mol. Struct.* **2010**, *972*, 2−10.

(75) Kütt, A.; Rodima, T.; Saame, J.; Raamat, E.; Mäemets, V.; Kaljurand, I.; Koppel, I. A.; Garlyauskayte, R. Yu.; Yagupolskii, Yu. L.; Yagupolskii, L. M.; Bernhardt, E.; Willner, H.; Leito, I. *J. Org. Chem.* **2011**, *76*, 391−395.

(76) Klamt, A. *COSMO-RS: From Quantum Chemistry to Fluid Phase Thermodynamics and Drug Design*; Elsevier Science, Ltd.: Amsterdam, The Netherlands, 2005.

(77) Bordwell, F. G. *Acc. Chem. Res.* **1988**, *21*, 456−463.

(78) Kaljurand, I.; Kütt, A.; Soovali, L.; Rodima, T.; Mäemets, V.; Leito, I.; Koppel, I. A. *J. Org. Chem.* **2005**, *70*, 1019−1028.

(79) Kütt, A.; Leito, I.; Kaljurand, I.; Soovali, L.; Vlasov, V. M.; Yagupolskii, L. M.; Koppel, I. A. *J. Org. Chem.* **2006**, *71*, 2829−2838.

(80) Because the experiments are carried out in the low polarity solvent CDCl₃, the term pH in this work should not be interpreted as referring to actual protonated solvent molecules in the solution, because their concentration is negligible. It should rather be understood in terms of the unified pH concept (Himmel, D.; Goll, S. K.; Leito, I.; Krossing, I. *Chem.—Eur. J.* **2011**, *17*, 5808−5826. Himmel, D.; Goll, S. K.; Leito, I.; Krossing, I. *Angew. Chem., Int. Ed.* **2010**, *49*, 6885−6888), where the unified pH is defined by the

absolute chemical potential of the proton in the solution and expresses the proton donicity of the overall solution, taking into account any acidic species in the solution (including of course protonated solvent molecules, if they exist).

(81) Kubasik, M.; Kotz, J.; Szabo, C.; Furlong, T.; Stace, J. *Biopolymers* **2005**, *78*, 87–95.

(82) Brown, R. A.; Marcelli, T.; De Poli, M.; Solà, J.; Clayden, J. *Angew. Chem., Int. Ed.* **2012**, *51*, 1395–1399.

(83) Fletcher, S. P.; Solà, J.; Holt, D.; Brown, R. A.; Clayden, J. *Beilstein J. Org. Chem.* **2011**, *7*, 1304–1309.

(84) Sairenji, S.; Akine, S.; Nabeshima, T. *Chem. Lett.* **2014**, *43*, 1107–1109.

(85) Cullen, W.; Turega, S.; Hunter, C. A.; Ward, M. D. *Chem. Sci.* **2015**, *6*, 625–631.

(86) Alder, R. W.; Bowman, P. S.; Steele, W. *Chem. Commun.* **1968**, 723–724.

(87) Alder, R. W.; Bryce, M. R.; Goode, N. C. *J. Chem. Soc., Perkin Trans. 2* **1982**, 477–483.

(88) Akine, S.; Sairenji, S.; Taniguchi, T.; Nabeshima, T. *J. Am. Chem. Soc.* **2013**, *135*, 12948–12951.

(89) Andréasson, J.; Pischel, U. *Chem. Soc. Rev.* **2015**, *44*, 1053–1069.

(90) de Silva, A. P.; Vance, T. P.; West, M. E. S.; Wright, G. D. *Org. Biomol. Chem.* **2008**, *6*, 2468–2480.

(91) de Silva, A. P.; McClenaghan, N. D. *Chem.—Eur. J.* **2004**, *10*, 574–586.

(92) Ahn, H.; Hong, J.; Kim, S. Y.; Choi, I.; Park, M. J. *ACS Appl. Mater. Interfaces* **2015**, *7*, 704–712.

(93) Siebler, C.; Erdmann, R. S.; Wennemers, H. *Angew. Chem., Int. Ed.* **2014**, *53*, 10340–10344.

(94) Knipe, P. C.; Jones, I. M.; Thompson, S.; Hamilton, A. D. *Org. Biomol. Chem.* **2014**, *12*, 9384–9388.

(95) Jones, I. M.; Lingard, H.; Hamilton, A. D. *Angew. Chem., Int. Ed.* **2011**, *50*, 12569–12571.

(96) Su, X.; Aprahamian, I. *Org. Lett.* **2011**, *13*, 30–33.

(97) Cho, J.-I.; Tanaka, M.; Sato, S.; Kinbara, K.; Aida, T. *J. Am. Chem. Soc.* **2010**, *132*, 13176–13178.

(98) Landge, S. M.; Aprahamian, I. *J. Am. Chem. Soc.* **2009**, *131*, 18269–18271.

(99) Okamoto, I.; Nabeta, M.; Minami, T.; Nakashima, A.; Morita, N.; Takeya, T.; Masu, H.; Azumaya, I.; Tamura, O. *Tetrahedron Lett.* **2007**, *48*, 573–577.

(100) Kanamori, D.; Okamura, T.-A.; Yamamoto, H.; Ueyama, N. *Angew. Chem., Int. Ed.* **2005**, *44*, 969–972.

(101) Dolain, C.; Maurizot, V.; Huc, I. *Angew. Chem., Int. Ed.* **2003**, *42*, 2738–2740.

(102) Kolomiets, E.; Berl, V.; Odriozola, I.; Stadler, A.-M.; Kyritsakas, N.; Lehn, J.-M. *Chem. Commun.* **2003**, 2868–2869.

(103) Mutter, M.; Gassmann, R.; Buttkus, U.; Altmann, K. H. *Angew. Chem., Int. Ed.* **1991**, *30*, 1514–1516.